Appl. Phys. B 65, 445–451 (1997)

Applied Physics B Lasers and Optics

© Springer-Verlag 1997

Numerical modeling of a XeCl laser excited by microwave discharge

A.V. Dem'yanov[1], **D. Lo**[2], **A.P. Napartovich**[1]

[1] Troitsk Institute of Innovative and Thermonuclear Research, Troitsk, Moscow Province, Russia
[2] Physics Department, The Chinese University of Hong Kong, Shatin, New Territories, Hong Kong

Received: 23 September 1996 / Revised version: 25 March 1997

Abstract. A comprehensive kinetic model for XeCl lasers excited by microwave discharge is formulated. In the model, the rate equations of reaction kinetics are solved self-consistently with the Boltzmann equation for electrons and the radiation transfer equation. The effective electric field strength needed in the solution of the Boltzmann equation is determined, by the energy balance argument, in terms of the microwave energy dissipated in the XeCl laser plasmas. The accuracy of the model is checked by comparing calculations with the experimental results reported by Christensen et al. in Optics Letters, **12**, 169 (1987). Reasonably good agreements in the peak output power and laser efficiency have been achieved. Model calculations also predict that an efficiency as high as 2.7% can be obtained once the conditions of the above-mentioned experiments have been optimized. From the consideration that the skin depth effectively limits the absorption length of the microwave pumping and hence the excitable volume, it is concluded that high input power densities ($\geq 2\,\mathrm{MW/cm^3}$) and higher gas pressures (between 3 and 10 atm) are the preferable conditions to achieve higher efficiency. Preliminary calculations on CCl_4 containing XeCl gas mixtures show that improvement in laser efficiency by several folds may be achieved as a result of the higher intrinsic efficiency of excimer formation.

PACS: 42.55; 52.80

XeCl lasers excited by pulsed discharge have been shown to have an efficiency of 5% at a per-pulse output energy of about 1 J [1]. This experimental result compares reasonably well with the theoretically predicted efficiency of 6% [2]. Uniform and stable discharge was assumed in the model calculations in [2]. The efficiency of scaled-up XeCl lasers with per pulse output of the order of 10 J ranges from 1% to 2% [3–5], which is much lower than the predicted value. The cause of the reduction of efficiency was attributed to discharge nonuniformity induced by inhomogeneity in preionization and in the discharge electrodes [6, 7], or by micro-instability followed by the formation of hot spots or hot filaments on the electrodes [8–13].

The electrodeless radiofrequency (RF) and microwave (MF) discharges of rare-gas halide excimer laser gas mixtures are more stable than those of dc pulsed discharges [14–24]. In particular, experiments on microwave-pumped XeCl lasers have so far demonstrated laser efficiencies of 6% [15], pulse repetition rates up to 8 kHz [16], and laser pulse durations of 6 ms [17]. Fluorescence pulse durations of 8 ms and efficiencies of 12.1% were also achieved for a microwave-pumped KrF lamp [18]. In spite of the promises of long pulse duration and higher efficiency in microwave-pumped excimer lasers, there has been few detailed parametric studies by theoretical modeling of microwave-pumped excimer lasers [29].

We have previously developed a fully comprehensive kinetic model for dc-pulsed discharge-pumped XeCl lasers [2, 25, 26]. This model is modified for microwave discharges as the effective electric field E_{eff} is used in the calculation of the electron energy distribution function (EEDF). Detail of the determination of E_{eff} is given in the next section. Detailed calculations were carried out to study the parameter space of interest for efficiency optimization. The results of the calculations indicate that because of the presence of a skin depth that practically limits the excitable volume, a high efficiency ($\geq 2.7\%$) can be achieved in conditions of high input power density ($\geq 2\,\mathrm{MW/cm^3}$) and higher gas pressures (between 3 and 10 atm).

1 Model description

The kinetic model used in the calculations is essentially the same one described fully in [2, 25, 26]. The model consists of a reaction kinetic module for the charged or neutral species of interest in the XeCl laser plasmas, a Boltzmann equation module for the calculations of the EEDF and the reaction rate constants, and the radiation transfer equation module that predicts the output emission for a particular resonator cavity arrangement. In the solution of the Boltzmann equation, the electron–electron collisions and the superelastic collisions (collisions with excited species) are taken into account so that the model is fully self-consistent.

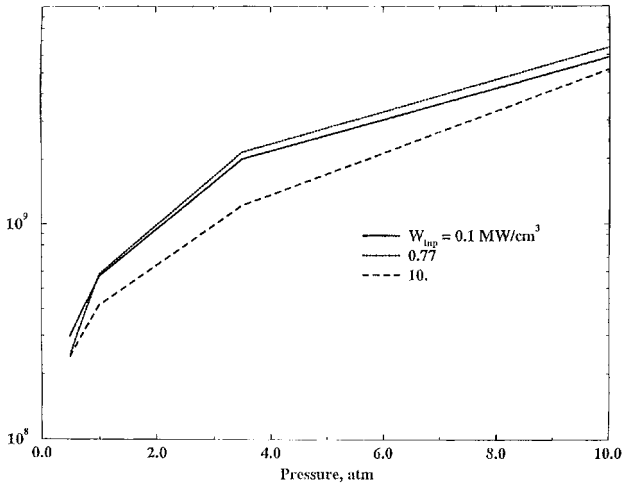

Fig. 1. Dependency of inelastic collisions frequency ν_U [s^{-1}] on gas pressures p [atm] for various input power densities: *solid line* $W_{in} = 0.1\,MW/cm^3$; *dotted line* $W_{in} = 0.77\,MW/cm^3$; *dashed line* $W_{in} = 10\,MW/cm^3$

In the case of the dc-pulsed discharge-pumped excimer lasers, the electron energy transfer (inelastic collisions) frequency ν_U is much larger ($\nu_U \approx 10^9\,s^{-1}$) than the oscillation frequency of the applied electric field. Hence, the solution of time-dependent Boltzmann equation is not necessary and a quasi-steady description of the EEDF is considered adequate. For most of the microwave-pumped excimer laser experiments reported in the literature [1, 4–22], the electric field frequency ranges from 1 to 3 GHz, which is of the same order of magnitude as ν_U at higher pressures. (See Fig. 1 which shows the variations of ν_U at different input power densities and gas pressure for a mixture ratio of He : Xe : HCl = 1000 : 10 : 1.) Hence, the quasi-steady description of the EEDF may not be entirely appropriate.

In the case when $\nu_U \ll \omega \ll \nu_m$, where ω is the angular frequency of the microwave field and ν_m is the momentum relaxation frequency, the time-averaged solution of the Boltzmann equation closely approximates that of the steady-state defined by the reduced electric field strength $E/N = E_0/N\sqrt{2}$, where E_0 is the amplitude of the microwave field [24, 27, 28]. The rate constants needed for reaction kinetic calculations can then be determined by solving the steady-state Boltzmann equation for an effective electric field $E_{eff} = E = E_0/\sqrt{2}$. Based on energy-balance arguments, the effective electric field E_{eff} is calculated from the experimentally measured absorbed pump power $W(t)$, i.e. by equating $W(t)$ to $eE_{eff}^2\mu_e n_e$, where e is the electronic charge, μ_e is the electron mobility, and n_e is the electron number density. This approach was adopted in [29] in the modeling of microwave-pumped XeCl lasers, and we call this the time-averaged approach in this paper. For XeCl laser mixtures at higher pressures, $\nu_U$is of the same order as ω (Fig. 1). Again, the use of the time-averaged approach may also be problematical.

The variation of the EEDF and the relevant reaction rate constants at different applied electric field frequencies (ω) were studied in detail for Ne : Xe : HCl gas mixtures [27] and for pure He and N_2 gases [28]. Calculations were performed for predetermined degrees of ionization and excitation, while requiring a balance of electron loss and production rates [27]. The results so obtained indicate that for $\nu_U \leq \omega$, the variation of EEDF, and hence also the mean electron energy and mobility, with the applied field frequency is not significant [27]. It is the reaction rates of the high-threshold processes (ionization and excitation of electronic levels) that are most sensitive to the change in the frequency of the applied field. Even so, for $\nu_u\omega$, the variation of these rates are no more than 20%. Therefore, an EEDF of reasonable accuracy can be obtained from the time-averaged solution to the Boltzmann equation for the experimental conditions given in [14–22].

Typically, our model calculations proceed as follows. In the initial time step, the number densities of the electron and plasma species (from preionization or otherwise), and the effective electric field E_{eff} (determined from the time history of the absorbed microwave power, which is known from experiments [29]) are taken as given. The EEDF is then determined from the time-averaged solution of the Boltzmann equation. Reaction rate constants and the electron mobility are calculated. These rate constants are used in the reaction kinetics module for the prediction of time-evolution of plasma species. The system of equations are solved by the Gear method [25]. The time step was adjusted to make sure that the variation in E_{eff} between time steps is small.

2 Comparison with experiments

To verify the accuracy of the model, comparison with experiments is necessary. A fairly complete set of experimental parameters are given in [16]. In the experiments, XeCl laser mixtures of He : Xe : HCl = 1000 : 10 : 1 at a pressure of 3.5 atm was housed in a 20-cm sapphire tube with inner diameter of 0.5 mm. The gain length is 15 cm. A concave total reflector (radius of curvature at 5 m) and a 80%-reflectance output mirror make up the resonator cavity. The round-trip optical loss is about 50% as a result of the poor quality of the sapphire tube. The time histories of both the microwave power and the XeCl laser pulse were measured. The frequency of the microwave is 915 MHz [16].

The results of our calculations are presented in Figs. 2–5. The time history of the microwave radiation absorbed in the active volume is shown in Fig. 2a (100% absorption). Both 100% absorption and 80% absorption were reported [16, 29]. A peak input power density of $0.77\,MW/cm^3$ is estimated from the dimensions of the sapphire tube described in [16]. Figure 2b shows the time history of XeCl laser at 100% and 80% absorption. Compared with the 100% case, the onset of lasing is late by 50 ns and the peak power is halved in the 80% case. But the peak power at about 100 W in the 80% case is in fairly good agreement with the experimental value of 80 W [16]. Time histories of various plasma species are shown in Fig. 3. It is seen that the maximum electron number density is about $7 \times 10^{14}\,cm^{-3}$. At the end of the pump pulse the ground-state number density of HCl is about one tenth of that at the beginning, which results in the early termination of the laser pulse. The electron energy branching at different channels as a function of time is shown in Fig. 4. It is observed from Fig. 4 that most of the electron energy is expended in elastic and excitation collisions with Xe. 200 ns into the pump pulse, almost all vibrational levels of HCl are accessed. This energy stored in the vibrational levels of HCl is later released to heat up the electrons.

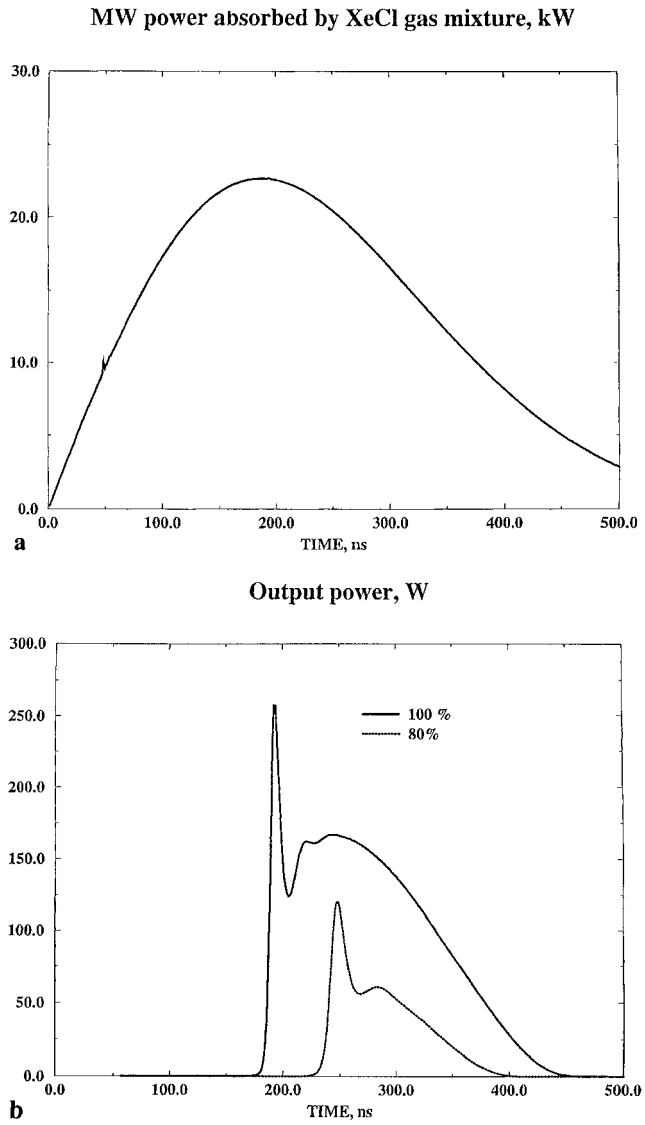

Fig. 2. a The time history of microwave radiation absorbed in the XeCl laser gas mixture. **b** XeCl laser output power for 100% absorption (*solid line*) and 80% absorption (*dotted line*)

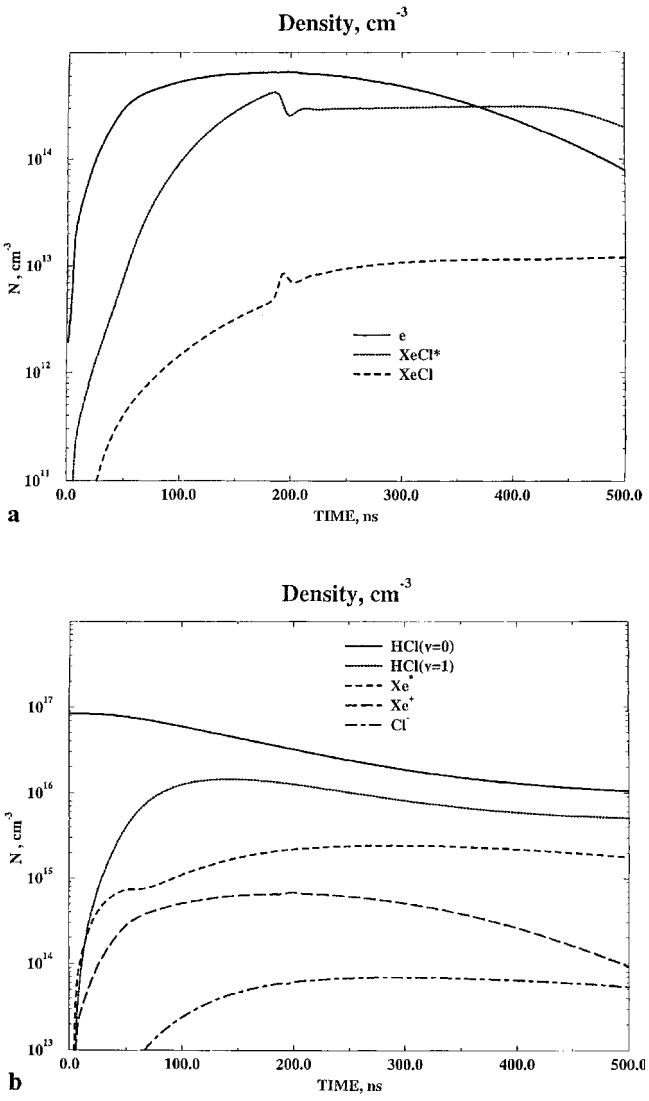

Fig. 3a,b. Time histories of several species in the XeCl laser plasma: **a** Electron, XeCl*, XeCl (ground state); **b** HCl ($v = 0$), HCl ($v = 1$), Xe*, Xe$^+$, Cl$^-$

Ishihara and Lin [29] have modeled the experiments reported in [16]. Their calculations of XeCl laser output power overestimated the measured values by 2.5 times. Our results (Fig. 2b) seem to better agree with the measurements. Upon close analysis of our model, it is observed that the accuracy of the EEDF affects the shape of the XeCl laser pulse. For the results presented here, the maximum difference of the EEDF between two time steps is set at 10^{-5}. As for the reaction kinetics, our model incorporate superelastic collisions of electrons with Xe* and vibrationally excited HCl [26]. The inclusion of these two processes reduces the number densities of Xe* and HCl (v) and thus effectively slows the reaction rates of ionization and attachment. The formation rate of XeCl (B) is also decreased as a result. Also, mixing of B and C states of XeCl molecules as well as the vibrational-translational relaxation of XeCl (B) state have been accounted for. These two processes serve to slow the formation rate of XeCl [B($v = 0$)]. We believe that the more elaborate description of collisional mixing of B and C states, the inclusion of superelastic collisions, and the more recent data of electron-quenching rate constants together contribute to the better fit with experimental results. Their relative contributions can be ascertained by relaxing the accuracy of the EEDF calculation between time steps and/or the elimination of one or more of the above reactions.

The skin depth L is calculated according to the formula

$$L = \frac{C}{\omega\kappa} \quad , \tag{1}$$

where ω is the angular frequency of the microwave field, κ is the extinction coefficient given as

$$\kappa = \left\{ -\frac{\epsilon}{2} + \left[\left(\frac{\epsilon}{2}\right)^2 + \left(\frac{2\pi\sigma}{\omega}\right)^2 \right]^{\frac{1}{2}} \right\}^{\frac{1}{2}} \quad . \tag{2}$$

Here ϵ and σ are the dielectric constant and the conductivity of the plasma [29]. In Fig. 5 we show the time history of

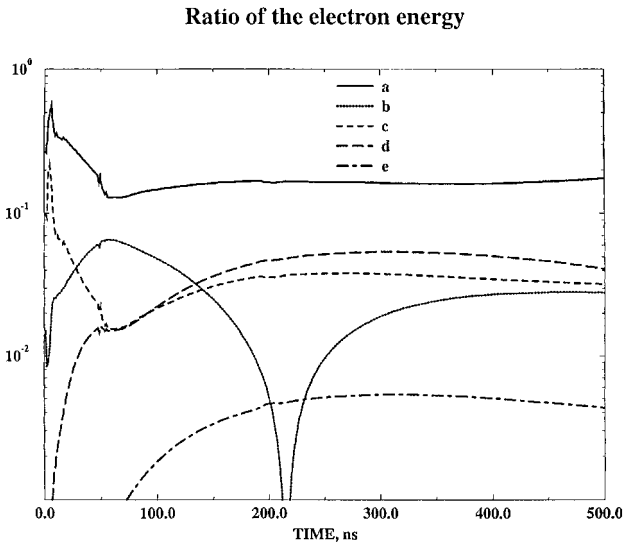

Fig. 4. The time variation of the electron energy branching via different channels: a – $Xe + e \rightarrow Xe^* + e$; b – HCl (v) + e– > HCl (v+1) + e; c – $Xe + e \rightarrow Xe^+ + 2e$; d – $Xe^* + e \rightarrow Xe^+ + 2e$; e – HCl (v) + e → H + Cl^-

the skin depth. When Fig. 5 is compared with Fig. 3a, the skin depth is seen to be largely influenced by the electron number density. The minimum skin depth at 5 mm corresponds in time to the maximum of the electron number density. In the experiments with microwave-pumped XeCl lasers [16], up to 100% absorption of the microwave power is reported for a sapphire tube with an inner diameter of 0.5 mm. Given that the minimum skin depth is 5 mm, one can safely assume that the gas mixture in the tube is uniformly excited. Deviation of the skin depth from 5 mm could adversely affect the laser efficiency because at too large a skin depth, part of the microwave pump pulse will transmit through the laser plasma, resulting in poor coupling efficiency, whereas at too small a skin depth, only the outer space of the gas mixture is effectively excited, leading to inhomogeneity in the active volume. Taking the ratio of the skin depth to the inner tube diameter to be optimal at 10 (recall that the absorption of microwave power is reported to be 100% [16]), one may be able to choose the gas pressure and pump power density in order to maximize the laser efficiency for a given sapphire tube and a given gas-mixture ratio. The time histories of the skin depth at a gas pressure of 10 atm and pump power densities of 0.1 MW/cm^3 and 10 MW/cm^3 are also shown in Fig. 5. The skin depth grows with pressure and diminishes with input power density.

3 Parametric study and efficiency optimization

Since microwave discharges of rare-gas halide laser mixtures have been recognized as more stable than dc-pulsed discharges, it is of interest to explore the optimum output performance of the microwave-pumped excimer lasers. With conditions typical of experiments (input power density, $W_{\text{in}} = 0.77$ MW/cm^3; pressure $p = 3.5$ atm; microwave frequency at 915 MHz; active medium length $L = 15$ cm) the laser efficiency is calculated as a function of the Xe content (Y_{Xe}) at three different reflectances (R) of the output mirror (Fig. 6). Figure 7 shows the results of the calculation of the laser efficiency as a function of R at three different HCl contents (Y_{HCl}). Figure 8 shows the laser efficiency for the cases with and without 50% optical loss. The optimum mixture ratio of He : Xe : HCl = 100 : 1 : 0.1 as observed from Figs. 6 and 7 corresponds to the experimental value in [16]. The optimum reflectance at $R = 80\%$ is also that used in [16]. Finally, the calculated efficiency of 0.6% for the case with 50% optical loss agrees well with the experimental result of 0.36% [16]. Note that an efficiency of 2.7% for the experimental conditions in [16] is predicted by our model (Fig. 8). This should be achievable if the poor-quality sapphire tube that contributes to the 50% optical loss is replaced.

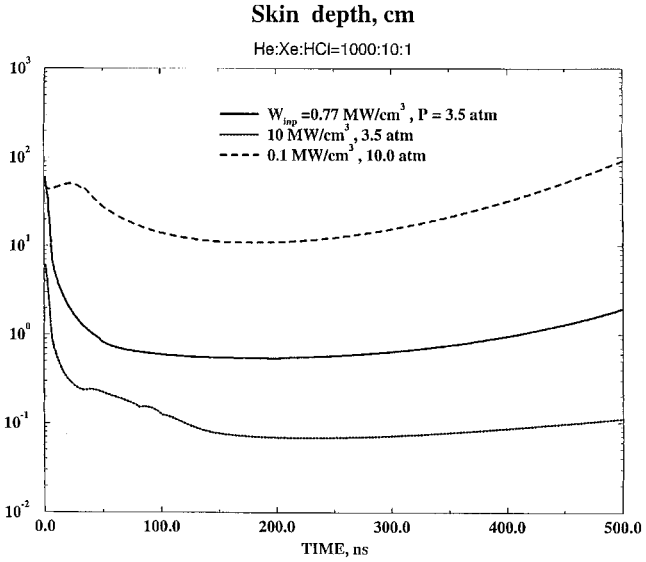

Fig. 5. The time histories for skin depth [cm] in gas mixtures He:Xe:HCl = 1000 : 10 : 1 for various input power densities and gas pressure: *dotted line* $W_{\text{in}} = 0.1$ MW/cm^3, $p = 10$ atm; *solid line* $W_{\text{in}} = 0.77$ MW/cm^3, $p = 3.5$ atm; *dashed line* $W_{\text{in}} = 10$ MW/cm^3, $p = 3.4$ atm

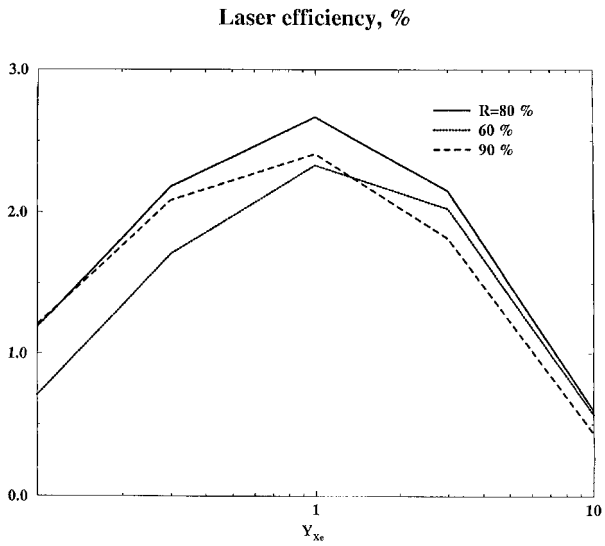

Fig. 6. Dependency of the laser efficiency [%] on Xe content (Y_{Xe}) in gas mixture He : Xe : HCl = 100 : Y_{Xe} : 0.1 for various reflectances (R) of the output mirror: *solid line* $R = 80\%$; *dotted line* $R = 60\%$; *dashed line* $R = 90\%$

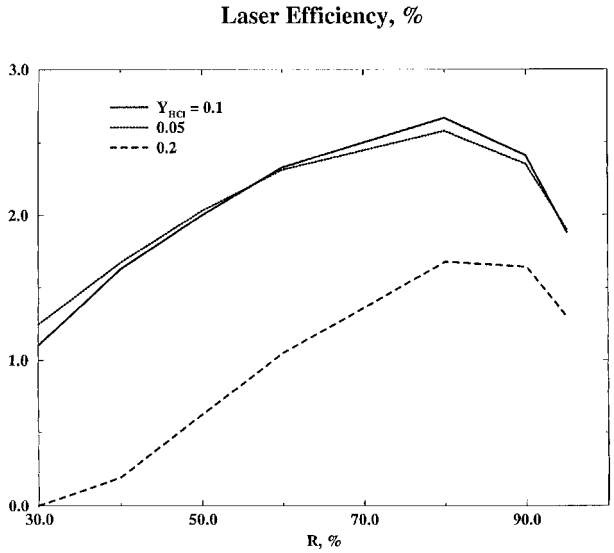

Fig. 7. Dependency of the laser efficiency [%] on the reflectances (R) of the output mirror for various HCl contents (Y_{HCl}) in gas mixture He : Xe : HCl $= 100 : 1 : Y_{\mathrm{HCl}}$ for: *solid line* $Y_{\mathrm{HCl}} = 0.1$; *dotted line* $Y_{\mathrm{HCl}} = 0.05$; *dashed line* $Y_{\mathrm{HCl}} = 0.2$

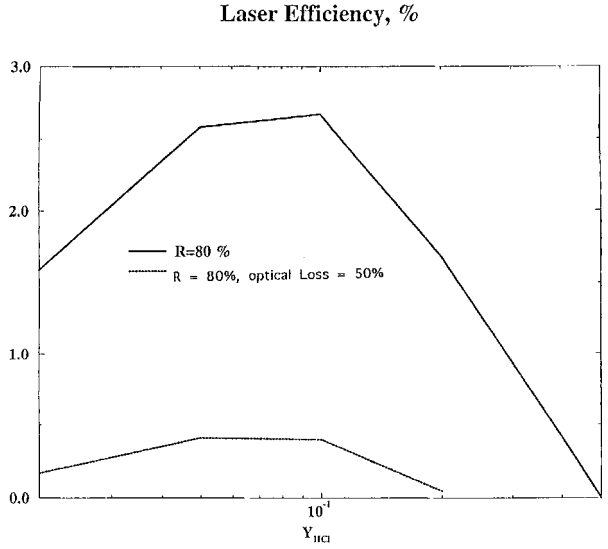

Fig. 8. Dependency of the laser efficiency [%] on HCl content (Y_{HCl}) in gas mixture ratio He : Xe : HCl $= 100 : 1 : Y_{\mathrm{HCl}}$ for cavities with or without 50% optical loss: *solid line* $R = 80\%$, no optical loss; *dotted line* $R = 80\%$, optical loss is 50%

Efficiency as high as $5\% - 6\%$ has been demonstrated for dc-pulsed discharge XeCl lasers [1, 2]. One may want to improve on the efficiency of the microwave pumped lasers, which is 2.7% according to our model calculations. In general, laser efficiency can be represented as the product of the kinetic efficiency (approximately the ratio of the excimer formation rate versus the ionization rate) and the resonator cavity efficiency as estimated by the Rigrod relationship [30]. The determining parameter of the resonator cavity efficiency is g_0/α, where g_0 is the small signal gain coefficient and α is the nonsaturable absorption coefficient. For the optimum coupling loss,

$$\Gamma_{\mathrm{op}} = (g_0\alpha)^{\frac{1}{2}} - \alpha = \frac{1}{2L}\ln\frac{1}{R} \quad , \tag{3}$$

the resonator cavity efficiency is equal to

$$\eta_{\mathrm{cav}} = \frac{\left[(g_0/\alpha)^{\frac{1}{2}} - 1\right]^2}{g_0/\alpha} \quad . \tag{4}$$

For typical conditions in microwave pumping, g_0/α is large enough (≈ 20 according to Fig. 9) for η_{cav} to be about the same as in the case of dc-pulsed discharge pumping [2]. Hence, the lower laser efficiency in the microwave-pump XeCl laser must be attributable to kinetic reasons. In our view, the increased fraction of electron energy loss to elastic collisions with He as compared to the Ne-buffered gas mixes used in [1, 2] as well as the less than optimum input power density used at the experimental pressure of 3.5 atm are the main causes. We also calculate the variation of the skin depth as functions of Y_{Xe} and Y_{HCl} (Fig. 10). The strong dependence of the skin depth on the HCl content is the result of the decrease in the electron number density caused by the accelerated attachment process.

To clarify the reasons for lower efficiency in microwave pumping, we calculate the laser efficiency as a function of pressure p at three different input power densities W_{in}. For $W_{\mathrm{in}} = 0.77\,\mathrm{MW/cm^3}$, the maximum laser efficiency occurs at $p = 1$ atm, where the excimers are quenched equally effectively by electrons and neutral species [25, 26]. We note, however, that a pressure of 3.5 atm was used in [16]. At increased W_{in}, the maximum laser efficiency occurs at higher p. Indeed for $W_{\mathrm{in}} = 10\,\mathrm{MW/cm^3}$, a laser efficiency as high as 0.45% is obtained at $p = 10$ atm (Fig. 11).

By contrast, the skin depth diminishes quickly with W_{in}. In Fig. 12, the minimum skin depth is depicted as a function of p for three values of W_{in}. For $W_{\mathrm{in}} = 0.77\,\mathrm{MW/cm^3}$ the skin depth is about 1 mm at $p = 1$ atm. This represents

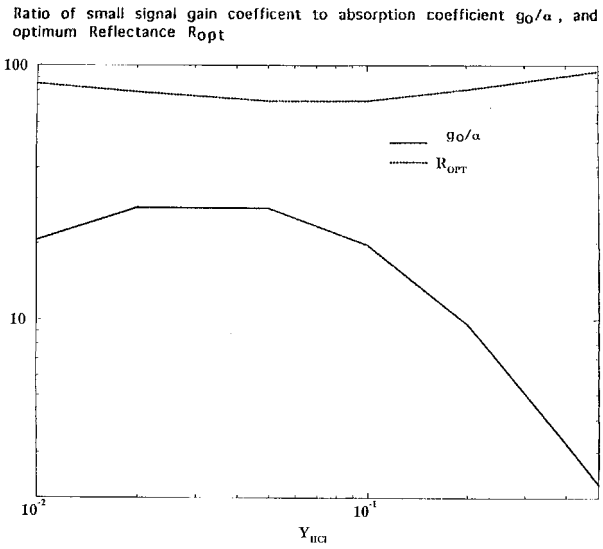

Fig. 9. Dependency of the ratio of the small-signal gain coefficient g_0 to the absorption coefficient α, and of the optimum reflectance of the output mirror on HCl content (Y_{HCl}) in gas mixture He : Xe : HCl $= 100 : 1 : Y_{\mathrm{HCl}}$

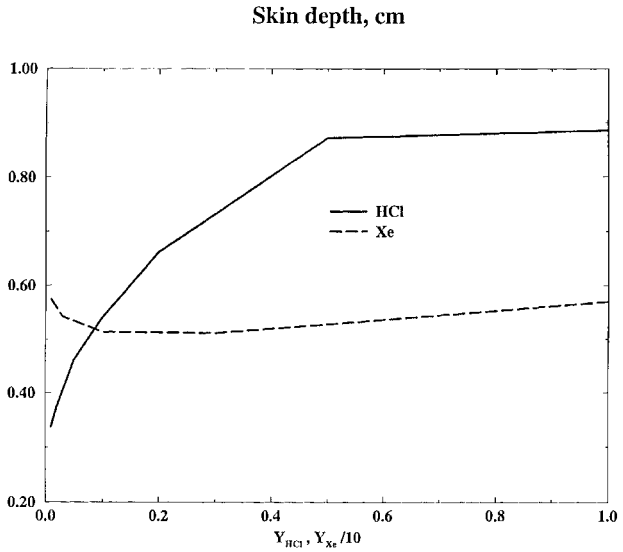

Fig. 10. Dependency of the skin depth (cm) on HCl content (Y_{HCl}) in gas mixture He : Xe : HCl = 100 : 1 : Y_{HCl} (*solid line*) and on Xe content (Y_{Xe}) in gas mixture He : Xe : HCl = 100 : Y_{HCl} : 0.1 (*dashed line*)

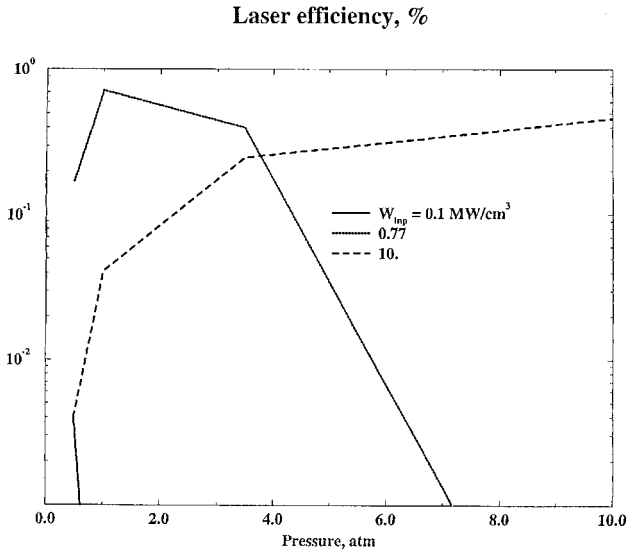

Fig. 11. Dependency of laser efficiency in gas mixture He : Xe : HCl = 1000 : 10 : 1 on gas pressure [atm] for various input power densities: solid line $W_{\mathrm{in}} = 0.1\,\mathrm{MW/cm^3}$; *dotted line* $W_{\mathrm{in}} = 0.77\,\mathrm{MW/cm^3}$; *dashed line* $W_{\mathrm{in}} = 10\,\mathrm{MW/cm^3}$

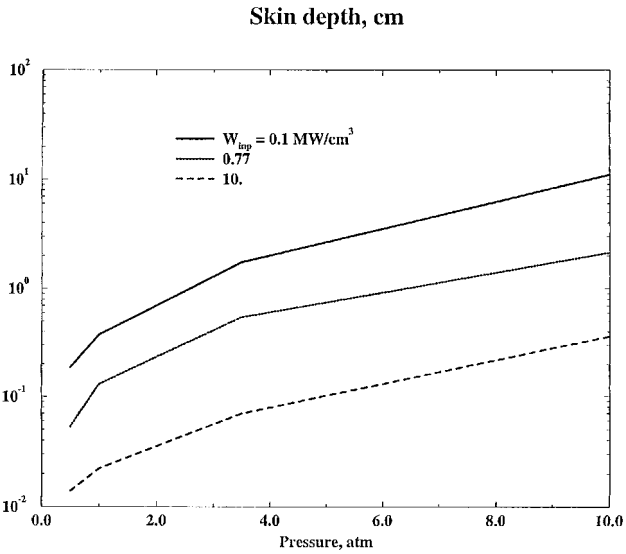

Fig. 12. Dependency of skin depth [cm] in gas mixture He : Xe : HCl = 1000 : 10 : 1 on gas pressure [atm] for various input power densities: solid line $W_{\mathrm{in}} = 0.1\,\mathrm{MW/cm^3}$; *dotted line* $W_{\mathrm{in}} = 0.77\,\mathrm{MW/cm^3}$; *dashed line* $W_{\mathrm{in}} = 10\,\mathrm{MW/cm^3}$

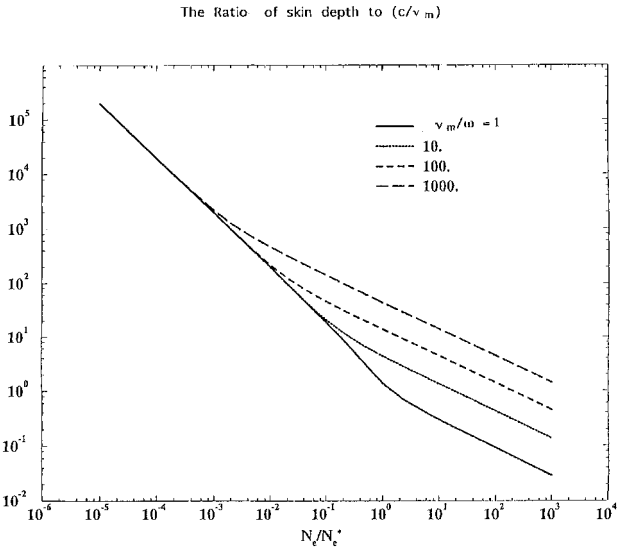

Fig. 13. Dependency of the ratio of the skin depth to c/ν_{m}, where c is the speed of light in vacuum and ν_{m} is the momentum relaxation frequency, on the normalized electron number density $n_{\mathrm{e}}/n_{\mathrm{e}}^*$, where $n_{\mathrm{e}}^* = \left[m_{\mathrm{e}}\left(4\pi e^2\right)\right](\omega^2 + \nu_{\mathrm{m}}^2)$ is the critical electron number density

a ratio of skin depth to inner tube diameter of 2, which is far smaller than the optimum ratio of 10 considered to be necessary for efficient ultilization of the microwave pump power (see Sect. 2 of this paper). With the optimum ratio of 10 taken as a rough guide and the assumption that the inner tube diameter is not smaller than 0.5 mm (from a literature survey on experimental work, the 0.5 mm diameter appears to be the smallest used in experiments), experimental conditions must be chosen so that a skin depth $\geq$ 3–4 mm can result. If this premise is agreed upon, one may opt to operate the microwave lasers at higher pressures in order to obtain higher efficiency (see Fig. 11). At such high pressures, high input power ($\geq 2\,\mathrm{MW/cm^3}$) must also be employed since lasing is not possible at higher p when pumping is delivered at low input power density (see Fig. 11). It is then safe to conclude that laser efficiency of the order of 3% can be obtained with an input power density in the range 2–10 $\mathrm{MW/cm^3}$ and p between 3 and 10 atm for a microwave frequency $\omega/2\pi$ of 915 MHz. This skin depth, of course, behaves differently at different $\omega/2\pi$. Such behavior is shown in Fig. 13.

4 Microwave pumped XeCl lasers using CCl_4 as halogen donor

We have performed a detailed model study of microwave pumped XeCl lasers in He : Xe : HCl mixtures. From previous work on dc-pulsed discharge-pumped XeCl lasers, it is known

that a higher performance can be obtained in Ne-buffered XeCl gas mixtures [1, 2]. Ne-buffered gas mixtures have indeed been used in experiments with microwave-pumped XeCl lasers [17, 22]. Operation at pressures as high as 17 atm was achieved [17]. However, experimental data and conditions as given in [17, 22] are not detailed enough for a model study.

An efficiency as high as 6% has been reported for a microwave pumped XeCl laser with CCl_4 as the halogen donor [15]. The halogen content in the mixture ratio of $Ne : Xe : CCl_4 = 300 : 60 : 1$ is higher than that used in dc-pulsed discharge [1–5]. a more detailed account of microwave experiments on CCl_4-containing XeCl laser mixtures can be found in [20], where a mixture ratio of $Ne : Xe : CCl_4 = 95 : 18 : 1$ was used. We have made a preliminary model study of microwave-pumped XeCl laser experiments in [20]. Laser efficiency as high as 28% is predicted by our model. Such a high efficiency is possible because 80% of the electron energy loss results in the excitation of Xe and CCl_4, both of which are precursors of XeCl (B), leading to a kinetic efficiency of 46%. This coupled with the resonator cavity efficiency of 60% (typical of a high g_0/α value at 25) could imply a potential laser efficiency of 28%. Other interesting features of microwave-pumped CCl_4-containing laser mixtures are the high electron temperature (≈ 6 eV) and the low electron number density (less than that of Cl^-). Both of these are the result of large attachment cross sections of CCl_4 at low electron energy. We did not pursue the study of microwave-pumped XeCl lasers with CCl_4 as the halogen donor further because of insufficient knowledge of the relevant cross-sectional areas of certain key kinetic reactions.

5 Conclusion

We have modeled microwave-pumped XeCl lasers with He : Xe : HCl mixtures using the time-averaged approach for the solution of the Boltzmann equation. Good agreement with experiments is obtained. Parametric studies show that efficiency of the order of 2.7% can be obtained for conditions typical of [16]. The prefered experimental conditions for higher efficiency are higher pressures (between 3 and 10 atm) and high input power densities ($\geq 2\,\mathrm{MW/cm^3}$) based on skin-depth considerations. Our preliminary study also indicates that higher efficiencies may be possible in gas mixtures with CCl_4 as the halogen donor.

Finally, we note that the skin depth expression used in the calculations in this work is an approximate one that assumes uniform plane waves impinging on some homogeneous plasma. This picture is, of course, far from accurate as the microwave is continuously attenuated during its propagation in the plasma, leading to a reduction in the power absorption and electron number density. The spatial inhomogeneity of the laser–plasma interactions must be treated by multi-dimensional (or at least one-dimensional) modeling, which, however, lies outside the scope of this work.

Acknowledgements. This work is supported in part by a CUHK Direct Grant.

References

1. J.W. Gerritsen, A.L. Keet, G.J. Ernst, J. Witteman: J. Appl. Phys. **67**, 3517 (1990)
2. A.V. Dem'yanov, I.V. Kochetov: Sov. J. Quant. Electron. **25**, 442 (1995)
3. K. McDonnald, P. Ingwerson, E. White, C. Young, E. Sergoyan, C. Fisher: *Record of IEEE 18th Power Modulation Symposium, Hilton Head, SC, 1988* (IEEE, New York 1988)
4. V.Yu. Baranov, V.M. Borisov, Yu. Stepanov: *Electric-discharge excimer lasers based on halogen-noble gases* (Energoatomizdat, Moscow 1988)
5. S. Bollanti, P.Di Lazzaro, F. Flora, G. Giordano, T. Hermsen, T. Letardi: Appl. Phys. B **50**, 415 (1990)
6. I.0. Blinov, A.V. Dem'yanov, I.V. Kochetov, A.P. Napartovich, A.A. Pastor, P.Yu. Serdobintsev, N.N. Subin: Sov. J. Quant. Electron. 18, 1531 (1988)
7. A. Schwaledissen, D. Loffhagen, Th. Hammer, W. Botticher: Appl. Phys. B **58**, 471 (1994)
8. D. Lo: Appl. Phys. B **49**, 535 (1989)
9. R.S. Taylor: Appl. Phys. B **41**, 1 (1986)
10. A. De Angelis, P. Di Lazzaro, F. Garosi, G. Giordano, T. Letardi: Appl. Phys. B **47**, 1 (1988)
11. M.J. Kushner: IEEE Trans. on Plasma Science **19**, 387 (1991)
12. W. Botticher: Proceedings of the XXI International Conference on Phenomena in Ionized Gases (ICPIG-XXI), Bochum, Germany (1993)
13. A.V. Dem'yanov, I.V. Kochetov, A.P. Napartovich, M. Capitelli, S. Longo: Sov. J. Quant. Electron. **25**, 645 (1995)
14. V.A. Vaulin, V.N. Slin'ko, S.S. Sulakshin: Sov. J. Quant. Electron. **18**, 1459 (1988)
15. S.V. Baranov, V.A. Vaulin, M.I. Lomaev, V.N. Slin'ko, A.S. Sulakshin, S.S. Sulakshin, V.Ph. Tarasenko: Kvantovaya (Moscow) **16**, 452 (1989)
16. C.P. Christensen, C. Gordon Ill, C. Moutoulas, B.J. Feldman: Optics Lett. **12**, 169 (1987)
17. P.J.K. Wisoff, A.J. Mendelson, S.E. Harris, J.F. Harris, J.F. Young: IEEE J. Quant. Electron. **18**, 1839(1982)
18. H. Kumagai, M. Obara: Appl. Phys. Lett. **54**, 2619 (1989)
19. C.P. Christensen, R.W. Waynant, B.J. Feldman: Appl. Phys. Lett. **46**, 321 (1985)
20. A.N. Didenko, V.M. Petpov, V.N. SIin'ko, A.S. Sulakshin, S.S. Sulakshin: Sov. Tech. Phys. Lett. **12**, 515 (1986)
21. C.P. Christensen, R.W. Waynant: Appl. Phys. Lett. **41**, 794 (1982)
22. A.J. Mendelson, R. Normandin, S.E. Harris, J.F. Young: Appl. Phys. Lett. **38**, 603 (1981)
23. U. Krause, J. Klienschmidt: J. Appl. Phys. **72**, 1437 (1992); H.H. Klingenberg, F. Gekat: App. Phys. B **54**, 205 (1992)
24. Yu.P. Raizer: *The Principles of Modern Physics of Gas Discharges Processes* (Nayka, Moscow 1980)
25. A.V. Dem'yanov, I.V. Kochetov, A.P. Napartovich et al.: Sov. J. Quant. Electron. **15**, 1147 (1985)
26. A.V. Dem'yanov, I.V. Kochetov, A.P. Napartovich, M. Capitelli, C. Gorse, S. Longo: Sov. J. Quant. Electron. **22**, 786 (1992)
27. C. Gorse, M. Capitelli, R. Celiberto, R. Winkler, J. Wilhelm: J. Phys. D: Appl. Phys. **23**, 1041 (1990)
28. N.A. Dyatko,, I.V. Kochetov, A.P. Napartovich: Fizika Plazmy **11**, 739 (1985)
29. T. Ishihara, S.-C. Lin: Appl. Phys. B **48**, 315 (1989)
30. Yu.A. Anan'ev: *Optical Resonators and Divergence Problems of Laser Radiation* (Nayka, Moscow 1979)